Smart Structures and Systems, *Vol. 28, No. 5 (2021) 631-642*
https://doi.org/10.12989/sss.2021.28.5.631

Numerical and experimental research on actuator forces in toggled active vibration control system (Part II: Experimental)

Sayyed Farhad Mirfakhraei [1a], Hamid Reza Ahmadi*[2] and Ricky Chan [3b]

[1] *Department of Civil Engineering, Seraj University, Tabriz, Iran*
[2] *Department of Civil Engineering, Faculty of Engineering, University of Maragheh, Maragheh, P.O. Box 55136-553, Iran*
[3] *Department of Civil and Infrastructural Engineering, Faculty of Civil Engineering, RMIT University, Melbourne, Australia*

(*Received February 22, 2020, Revised June 27, 2021, Accepted August 27, 2021*)

Abstract. In this research, new toggled actuator forces were proposed. For this purpose, numerical and experimental investigation of the installation of the actuator in a toggle configuration for the decreasing of active control forces in engineering structures has been carried out. In the first part, numerical studies were investigated. In addition to numerical research on the effects of the toggle configuration on actuator forces, an experimental investigation has been carried out by building a table model of the mentioned system. The algorithm of the system is LQR, and ATmega328 has been used as a control platform. Comparing results through the experimental and numerical processes express high matching that relies on mitigating control forces in the toggled active model. Based on the results, a significant reduction in actuator forces through using the proposed toggle configuration.

Keywords: control forces; experimental investigation; structural active vibration control; toggled actuator

1. Introduction

Active control systems have been employed on structures to preserve them against seismic loads about twenty years ago (Yang and Soong 1988, Housner *et al*. 1997, Xu and Teng 2002, Spencer and Nagarajaiah 2003, Xu *et al*. 2014, Dinh *et al*. 2016, Muthalif *et al*. 2017, Zhan *et al*. 2017, Braz-Cesar and Barros 2018, Yanik 2019). Structural engineers were able to design taller and more flexible structures by utilizing advanced analytical software and materials with high strength (Yang and Soong 1988, Hejazi *et al*. 2016, Fu 2018, Ahmadi and Anvari 2018a, Bayat *et al*. 2019). More strength and ductility will require in the structure if there is intensive excitation on it (Rabczuk *et al*. 2007, Gandomi *et al*. 2011, Bayat *et al*. 2018, Hasni *et al*. 2017, Ahmadi and Anvari 2018b). The latter method is costly. Using more sizeable sections in the frame creates even more excitation loads onto the members, resulting in even larger sections (Shokouhian *et al*. 2016, Najafabadi *et al*. 2020). Utilizing smart structures can cure this latter dilemma showing one of their main advantages (Alavi *et al*. 2018, Bisheh *et al*. 2019, Alkayem *et al*. 2019, Bayat *et al*. 2020a). The past investigations and their practical implementations on structures to preserve the buildings against excitation loads prove the capability of smart structures. (Ahmadi *et al*. 2015, Bayat *et al*. 2020b). Furthermore, when multiple modes are dominant in the structures in the response, it requires a more adaptive and robust system to prevent the structure from powerful tremors and destruction (Cheng *et al*. 2008, Cao and Qiao 2009, Cao *et al*. 2014). Moreover, the number of actual installed active control systems throughout the world has been presented (Yamazaki *et al*. 1992, Abe and Fujino 1994, Spencer and Sain 1997, Cao *et al*. 1998, Kareem *et al*. 1999, Ikeda *et al*. 2001, Yamamoto *et al*. 2001, Ricciardelli *et al*. 2003, Park *et al*. 2006, Tian *et al*. 2017, Gharebaghi and Zangooei 2017, Bagha and Modak 2017, Majeed *et al*. 2018). Also, Cheng's research team has developed utilizing the active control system in the massive civil engineering structures (Cheng *et al*. 2008). To gain significant trust and security in high-rise buildings worldwide, utilizing active control systems would be inevitable. (Yang and Soong 1988).

Doubtlessly, gaining optimum control force in preparation for the structural response is one of the most important requirements in active control systems. The price of actuators and their maintenance costs are very expensive. Also, they need a considerable amount of electricity during their performance (Liu *et al*. 2003, Amini and Tavassoli 2005, Park *et al*. 2008). Recently, researchers tried to lower the control forces in these systems to mitigate the structural response as a productivity factor (Cheng *et al*. 1988, Pantelides and Cheng 1990, Fisco and Adeli 2011, Miah *et al*. 2015). Moreover, the location of implementation of the actuator in active control systems is very important, and the reduction of the structural response has been presented (Pantelides and Cheng 1990, Xu and Teng 2002, Liu *et al*. 2003, Amini and Tavassoli 2005, Rao and Sivasubramanian 2008, He *et al*. 2015).

There is a configuration known as a toggle, which is an

*Corresponding author, Ph.D., Associate Professor,
E-mail: ahmadi@maragheh.ac.ir
[a] Ph.D., E-mail: mirfakhraei@seraj.ac.ir
[b] Ph.D., E-mail: ricky.chan@rmit.edu.au

ISSN: 1738-1584 (Print), 1738-1991 (Online)

efficient sketch using in viscous damper implementing in a structural system. Using this pattern and putting some elements, they dissipated the conventional earthquake excitation and preserved the structure against the tremor. (Soong and Dargush 1997, Council 2000, De Domenico and Ricciardi 2018). It has been expressed that fluid viscous dampers can profoundly expand the damping ratio and lower the structural excitations (Hwang *et al*. 2004, Reinhorn *et al*. 2005, Bayramoglu *et al*. 2014, Ras and Boumechra 2016, Lu *et al*. 2018). Furthermore, one can find the actual installation of these dampers in the report (Soong and Spencer 2002). On the other hand, in a stiff structure, the structural responses are tiny compared to the flexible one. Consequently, installing viscous dampers in structures with high stiffness is less productive than flexible structures.

Considering the last-mentioned problem, to increase the displacements and velocities in dampers, some patterns for their installation positions have been recently investigated. The "toggle-brace-damper" pattern has been introduced by Taylor in U.S. Patent Nos. 5870863 and 5934028, 1996 (Taylor 1999a, b). Also, research related to the "toggle-brace-damper" pattern has been performed by (Constantinou *et al*. 2001). They showed in this investigation that utilizing the latter system can enlarge the axial displacements of the damper as well as the energy dissipation thru a cyclic loading carried out by shaking table tests in a SDOF (Single Degree of Freedom) steel frame. The necessity of having adequate architectural spaces in designing of buildings, a similar system to the prior one known as the "scissor-jack-damper" system has been introduced (Sigaher and Constantinou 2003). Similarly, the presented pattern magnified the damper displacements and velocity and enhanced the energy dissipation in the structure. The number of the actual installation of this system have been presented by Constantinou *et al*. (2001). The practical example of the latter system is located on 111 Huntington Avenue in Boston, Mass., in which a lower toggle system is directly pinned to the beam-column joints, which is different than the pattern presented by Constantinou (Constantinou *et al*. 2001). Additionally, the influence of the lower and upper toggle patterns in the latter system, as well as the facilitation of the practical damper implementation in the frame, have been studied by Hwang *et al*. (2005).

Part I of this research, the theoretical studies of the proposed toggled actuator were investigated (Mirfakhraei *et al*. 2020). In part II, which is the experimental part of this research, a small frame, as shown in Fig. 1, was built, having the toggle pattern and complete set of the active control system. As denoted in part I of the study, the latter model is a smart structure that consists of a rotational actuator which installed in the upper toggle system directly connected to the beam-column joints through a unique mechanism, an accelerometer as a sensor located on top of the structure and surcharge on the ceiling. The assembly has a controller platform connected to the computer that sends the signals to the actuator and receives them from the accelerometer using Matlab® software. The assembly was located on the benchtop shaking table, producing the known famous earthquake acceleration. Unlike the passive systems, this experimental research is related to the active control system and intends to discover the effects of the toggle configuration in mitigation of the active control forces and stabilizing the structure under the excitation.

The experimental results show that an active control system can be carried out using the set of the benchtop shaking table, proper small scale frame, the actuator, the controller platform ATmega328, the analogue accelerometers known as ADXL335, and the algorithm programmed in Matlab® software. Moreover, the experimental results prove the effectiveness of the toggle coefficient Ω in the reduction of the control forces in the active toggle control system as well as verification of the vibration reduction of the control forces. Additionally, the experimental outcomes confirm the integrity of the observer technique and also show that this type of experimental process is more economical compared with the full-scale model.

2. Experimental model

2.1 Frame

In this research, it was decided to use the small-scale model so that the experiment test could be carried out utilizing a proper small shaking table. As is clear from Fig. 1, the active toggle control experimental model was built manually in the laboratory of RMIT University. This model consists of four columns and a rigid ceiling connected to the columns. The material of the columns and ceiling are made of aluminium and timber, respectively. The columns, which are attached to the timber base, were selected to be flexible enough to be vibrated easily during the shaking on the shaking table. The ceiling was chosen rigid enough to transverse the vibration consistently to the four columns and follow the theoretical concept of the single-storey frame vibration. The connections of the columns with the ceiling

Table 1 Frame specifications

Explanation	Symbol	Value	Unit
Span length	L	0.346	m
Width	W	0.202	m
Height	H	0.258	m
Lower brace	l_1	0.150	m
Upper brace	l_2	0.294	m
Angle between lower brace and floor	ϕ_1	17.5	degree
Angle between upper brace and right column	ϕ_2	43.6	degree
Angle of control force	ϕ_3	33.9	degree
Mass	M	1.094	kg
Stiffness	K	169.4	N/m
Damping	C	0.184	Ns/m
Toggle coefficient	Ω	1.93	—

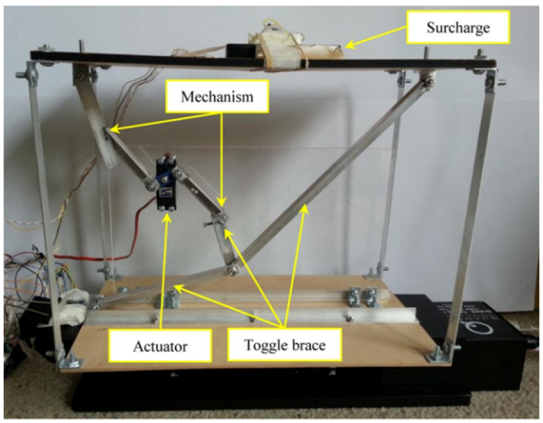

Fig. 1 Experimental model

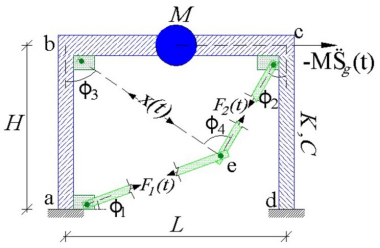

Fig. 2 Existing forces of toggle in active control system

and floor are considered the fixed end. The specifications of the experimental frame are indicated in Table 1.

In the above-mentioned table, toggle coefficient Ω has been calculated using Eq. (1) and considering the relevant values for the experimental model. Also, the stiffness and damping of the model structure can be obtained in the following section.

$$\Omega = Sin\varphi_3 + \frac{Cos(\varphi_1 - \varphi_3)}{Cos(\varphi_1 + \varphi_2)} Sin\varphi_2 \quad (1)$$

where, the angles of ϕ_1, ϕ_2, and ϕ_3 have been shown in Fig. 2.

2.2 Stiffness and damping of the model

The stiffness and damping of the model structure can be obtained by using the free vibration test (Mahdavi *et al.* 2012, Chopra 2017, Ahmadi *et al.* 2019). The free vibration of the model is shown in Fig. 3.

For finding the damping ratio, the information related to the desirable peak, time, and acceleration should be selected and obtained from Fig. 3. The relevant information is indicated in Table 2.

Table 2 Required information for calculating of damping ratio

Peak	Time (sec)	Acceleration (g)
1	12.4	0.275
11	17.45	0.18

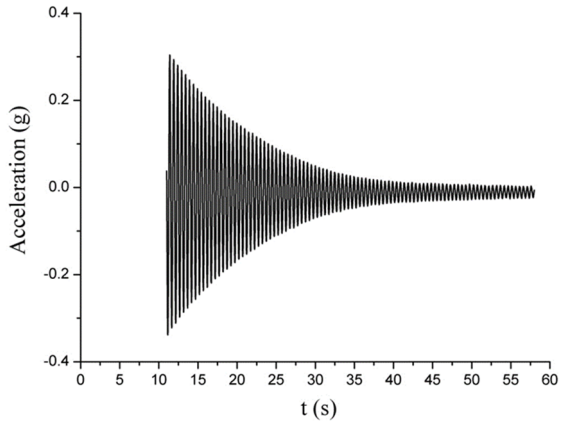

Fig. 3 Free vibration of the model

Also, the natural period of the model can be calculated from the free vibration test. Using Fig. 3 and Table 2, the natural period T_D can be derived as follows

$$T_D = \frac{T_{11} - T_1}{N} \quad (2)$$

In the above-mentioned formula, N is the number of peaks between T_1 and T_{11}, which is 10. Therefore, using Eq. (2), the natural period of model T_D = 0.505 sec is obtained. The damping ratio of the model structure can be calculated using the following formula.

$$\zeta = \frac{1}{2\pi N} ln \frac{\ddot{S}_1}{\ddot{S}_{11}} \quad (3)$$

Using Table 2, the damping ratio can be calculated from the above-mentioned formula. Therefore, after substituting the relevant values in Eq. (3), ζ = 0.67%, and after finding the damping ratio, the natural circular frequency can be calculated as follows

$$\omega_n = 2\pi / T_D \quad (4)$$

By substituting T_D = 0.505 sec the natural circular frequency becomes ω_n = 12.4 rad/sec. Then, the stiffness and damping of the model structure can be derived from the following equations, respectively.

$$K = M{\omega_n}^2 \quad (5)$$

$$C = \zeta(2\sqrt{MK}) \quad (6)$$

In the above formulas, M is the assumed lump mass of the model located at the ceiling and indicated in Table 1. Then, replacing the relevant values in Eqs. (5) and (6) results in K = 169.4 N/m and C = 0.184 N.sec/m.

2.3 Toggle configuration

As denoted before, the toggle configuration is installed in the frame. Since a suitable linear actuator fitting to the model and working fast enough in time intervals smaller

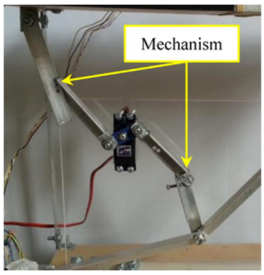

Fig. 4 Mechanism in the toggle configuration to convert rotation movement to linear

than one second was not found, a servo motor was installed instead of the linear actuator. The servo motor works fast enough and is suitable for this experiment. However, it creates a rotational movement and also has high stiffness, which prevents the frame from vibrating during uncontrolled shaking. For removing these disadvantages, a mechanism has been implemented in the toggle configuration to convert the movement from the rotation to linear and to also allow the frame some free shaking while it is attached to the servo motor. This mechanism has been shown in Fig. 4.

2.4 Actuator

As discussed in the previous section, the servo motor with the specifications indicated in Table 3 has been installed in the model as the actuator, shown in Fig. 5. This actuator is connected to the toggle system and the frame by the two members, as indicated in Fig. 5 (Blue Bird Model 2015). These two members consist of the explained mechanism. All the connections between the actuator and the latter members are joint connections. The installed actuator is connected to the controller platform, which sends the control signals to the actuator. The controller platform will be explained in the next section.

Table 3 Specifications of the servo motor (actuator)

Dimension	40.5 × 20 × 38 *mm*
Weight	51 grams
Torque At 4.8V	6.4 kgcm
Torque At 6.0V	7.2 kgcm
Speed At 4.8V	0.13 sec/60° at no load
Speed At 6.0V	0.10 sec/60° at no load

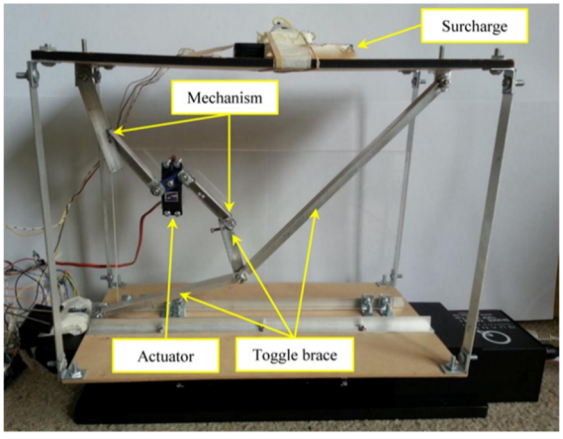

Fig. 5 Servo motor (actuator)

2.5 Controller platform

The controller platform used in this experimental test is the electronic platform known as ATmega328. It includes 14 digital input/output pins, 6 analogue inputs, a 16 MHz ceramic resonator, a USB connection, a power jack, an ICSP (In-Circuit Serial Programming) header, and a reset button. This platform has specific software and must be installed on the appropriate computer. It can be easily connected to the computer and linked with the MATLAB® software. This linkage with the MATLAB® software is very important, because the control signals calculated by the relevant algorithm are applied to the actuator through this platform. Also, it has to be mentioned here that the actuator is connected to this platform. The specifications of the

Fig. 6 Controller platform ATmega328

Table 4 Specifications of the controller platform ATmega328

Microcontroller	ATmega328
Operating voltage	5 V
Input voltage (recommended)	7-12 V
Input voltage (limits)	6-20 V
Digital I/O pins	14 (of which 6 provide PWM output)
Analog input pins	6
DC current per I/O pin	40 mA
DC current for 3.3V pin	50 mA
Flash memory	32 KB (ATmega328) of which 0.5 KB used by bootloader
SRAM	2 KB (ATmega328)
EEPROM	1 KB (ATmega328)
Clock speed	16 MHz
Length	68.6 mm
Width	53.4 mm
Weight	25 *g*

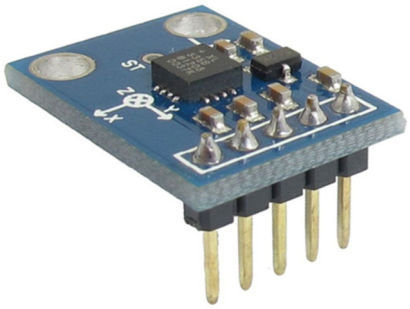

Fig. 7 Accelerometer used for experimental model

controller platform ATmega328 are indicated in Table 4. Also, the photo of this controller is shown in Fig. 6.

2.6 Accelerometer

In this research, the analogue accelerometer known as ADXL335 has been utilized in the experimental model for measuring the excitations. The photo of this accelerometer is shown in Fig. 7. This accelerometer is an analogue accelerometer, which has been implemented at both the top of the model and the shaking table. This type of accelerometer is compatible to synchronize with the selected controller platform.

The specifications of the accelerometer as mentioned earlier are as follows:

- Dimension 4 mm × 4 mm × 1.45 mm
- Ability to measure 3-Axis ±3 g acceleration
- Single-supply operation: 1.8 V to 3.6 V
- 10,000 g shock survival
- Measurement bandwidth for X and Y axis from 0.5 to 550 Hz

2.7 Shaking table

The shaking table used in this experimental test is called Shake Table I-40, made by the Quanser Company. It has some pre-loaded acceleration profiles of real earthquakes, such as Northridge, El-Centro, Mendocino, and Kobe. More information can be accessed on Quanser's website. This shaking table is connected to the computer through its specific software, named Quarc v2.4. This software can create a linkage with MATLAB® software. The photo and specifications of this shaking table are shown in Fig. 8 and Table 7, respectively.

Setting up the Shake Table I-40 for MATLAB®/ Simulink® needs additional components, as follows.

2.8 Q2-USB data acquisition device

Through the ground-breaking Quanser USB data acquisition technology, reliable real-time performance is delivered via a USB interface. Q2-USB data acquisition device offers an extensive range of hardware features and software support capabilities. The photograph of this device is shown in Fig. 9. The technical specifications of this device are indicated in Table 6, further below.

Fig. 8 Shaking table used for experimental test

Table 5 Technical specifications of Shake Table I-40

Dimensions (H×L×W)	57.5 cm × 12.7 cm × 7.62 cm
Total mass	5.88 kg
Payload area (L×W)	43.2 cm × 10.2 cm
Maximum payload at 1.0 g	1.5 kg
Travel	± 20 mm
Operational bandwidth	20 Hz
Peak velocity	46.9 cm/s
Peak acceleration	1.13 g
Lead screw pitch	10 mm/rev
Brushless servomotor power	70 W
Maximum continuous current	3 A
Motor maximum torque	3.53 N.m
Encoder line count (in quadrature)	8192 counts/rev
Encoder linear resolution (in quadrature)	1.22 μm/count
Accelerometer range	± 49 m/s²
Accelerometer sensitivity	1.0 g/V

Fig. 9 Q2-USB data acquisition device

2.9 VoltPAQ-X2 linear voltage amplifier

The VoltPAQ-X2 is a linear voltage-controlled amplifier, which is very suitable for research needs in all complex control areas. Its design is based on achieving high performance with Hardware-In-The-Loop (HIL) implementations. The photograph of this device is shown in Fig. 10. The technical specifications of this device are indicated in Table 7 below.

Table 6 Q2-USB technical specification

System requirements	Type A USB 2.0 connector (USB 2.0 driver is required)
Board dimensions (L×W×H)	8.5 cm × 10.2 cm × 1.8 cm
Analog inputs	
Number of channels	2
Resolution	12-bit
Input range	± 10 V
Conversion time	250 ns
Input impedance	10 MΩ
Maximum full scale range (FSR) error	± 10 LSB
Analog outputs	
Number of channels	2
Resolution	12-bit
Output range	± 10 V
Slew rate	3.5 V/μs
Conversion time	10 μs
DC output impedance	0.5 Ω
Short-circuit current clamp	20 mA
Maximum capacity load stability	4000 pF
Non-linearity	± 1 LSB
Maximum full scale range (FSR) error	± 12 LSB
Maximum load for specified performance	2 kΩ
Digital inputs	
Number of digital I/O lines	8
Input low / high	0.66 V / 2.31 V
Input leakage current	± 2 μA
Digital outputs	
Number of digital I/O lines	8
Output low / high	0.4 V / 2.40 V
Maximum drive current	± 4 mA
Encoder inputs	
Number of encoder inputs	2
Input low / high	0.66 V / 2.31 V
Input leakage current	+/– 2 μA
Maximum A and B frequency in quadrature	6 MHz
Maximum count frequency in 4x quadrature	10 MHz
PWM outputs	
Number of PWM outputs	2
Output low (max) / high (min)	0.40 V / 2.40 V
Minimum frequency	2.385 Hz
Maximum frequency	40 MHz
Bits resolution	16 bits

Fig. 10 VoltPAQ-X2 linear voltage amplifier

Table 7 Technical specification for VoltPAQ-X2 linear voltage amplifier

Dimensions (L×W×H)	39 cm × 33 cm × 10 cm
Mass	4.4 kg
Amplifier type	linear
Number of outputs	2
Load continuous current output	± 4 A
Amplifier gain	1 V/V or 3 V/V (gain selectable)
Current sense	1 V/A
Amplifier command	± 10 V
Number of analog inputs	4
Supply AC voltage	100 - 127 V or

2.10 Control algorithm

The control algorithm for this experimental test has been programmed in MATLAB® software. This program acts based on LQR (Linear Quadratic Regulator), and the pole placement algorithm explained in previous sections. Eventually, the control forces determined by this algorithm are applied to the structure through the controller platform and via the actuator. The main stages of the control algorithm program are as follows:

- Definition of the communication port between Matlab® software and controller platform ATmega328.
- Inputting of the number of sensors.
- Verification of the calibration matrix.
- Creation of the button to cease data collection.
- Creation of the button to close the serial port.
- Delineation of the time buffer duration.
- Creation of the variables to store the acceleration data for each sensor.
- Inputting of values for L, H, and l_1.
- Calculation of maximum values for ϕ_1 and ϕ_2.
- Inputting of the available ϕ_1.
- Checking of the toggle validation criterion, i.e., $\phi_1 + \phi_2 < 90°$.
- Calculation of the toggle coefficient Ω.
- Inputting of values for M, K, and C.
- Inputting of matrices α, β_u, β_r, κ, and λ.
- Creation of the observability matrix for the system.
- Checking of the observability of the system.

- Finding of the gain matrix of the observer in the closed-loop system.
- Derivation of the controlled displacements of the system.
- Calculation of the control forces for the system.
- Calibration of the system and applying the control forces to the system as a rotation angle to the servo.

3. Experimental model

3.1 Set-up of the experimental test

The set-up of the experimental test for verifying the validity of the toggle coefficient is explained by the following steps:

a. A ready-to-use personal computer having Windows7 Operating System relevant to the software.
b. Installing Matlab® software with one of the versions of R2012 to 2013 into the same computer.
c. Installing the proper Microsoft Compiler C++ in the computer.
d. Installing Quarc v2.4 software for running the shaking table, changing the frequencies, choosing the different earthquake excitations, and exporting the required data. A screenshot of Quarc software has been shown in Fig. 11.
e. Installing the platform controller software to the computer.
f. Having the algorithm in Matlab® code ready to run and to interface with the controller platform.

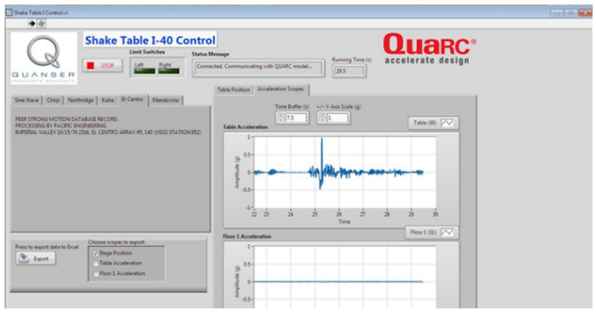

Fig. 11 A screenshot of Quarc software

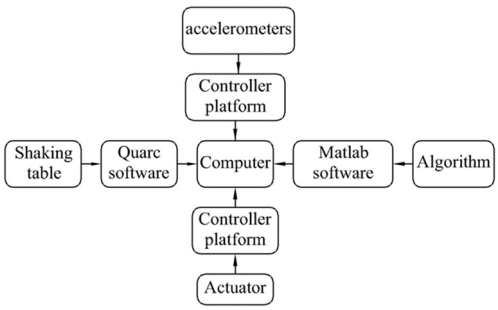

Fig. 12 Schematic depiction of connections of the devices for the experimental test

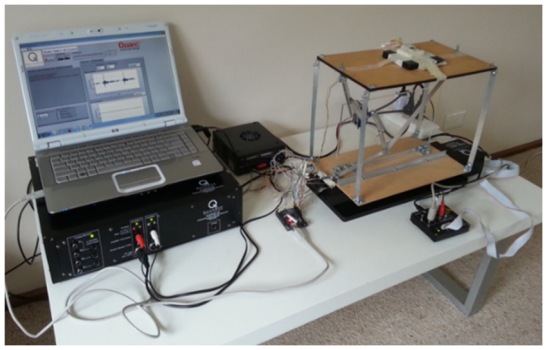

Fig. 13 A photograph of experimental test device connections

g. Implementing an accelerometer at the top of the model.
h. Implementing another accelerometer at the top of the shaking table.
i. Attaching the model into the shaking table used the proper screws.
j. Connecting the computer, analogue accelerometer, actuator, shaking table, and controller platform with each other as indicated schematically in Fig. 12. Also, a photograph related to the experimental test connections of different devices is provided in Fig. 13.

3.2 Experimental test performance

After setting up the plant and plugging the relevant devices into the electricity source, the performance of the experimental test is explained through the following steps:

a. Levelling of the shaking table.
b. Running of the computer and Matlab® software.
c. Calibration of the shaking table by running the specific program in Matlab® software.
d. Calibration of the two accelerometers by running the specific program in Matlab® software.
e. Running of the control algorithm program as described in Section 2.10.
f. Visual checking of the accelerometer measurements in the computer screen to show as zero. This means that the accelerometers read zero acceleration from the shaking table and the frame while the experimental plant is at rest.
g. Running of the Quarc software to set up the shaking table.
h. Selection of the desired earthquake acceleration among the preinstalled earthquake accelerations in Quarc software. These earthquakes are 1979 Imperial Valley–El Centro M (6.5), 1992 Mendocino M (7), and 1995 Kobe (6.9) indicated in Figs. 14 to 16, respectively.
i. In this step, the shaking table applies the real earthquake excitations to the system, the shaking table starts to shake, and the system responds to the excitations based on its algorithm.
j. During the excitation, accelerations related to the shaking table and the top of the frame are measured

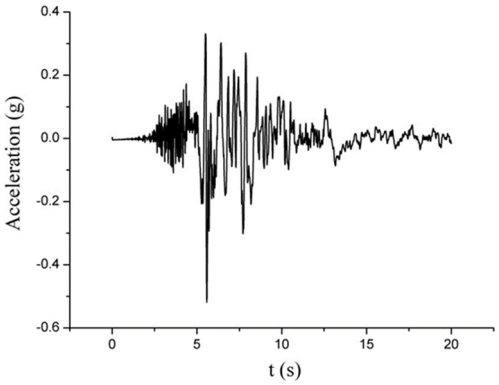

Fig. 14 1979 El Centro earthquake accelerations

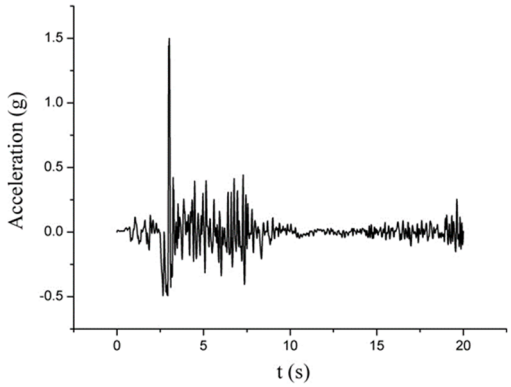

Fig. 15 1992 Mendocino earthquake accelerations

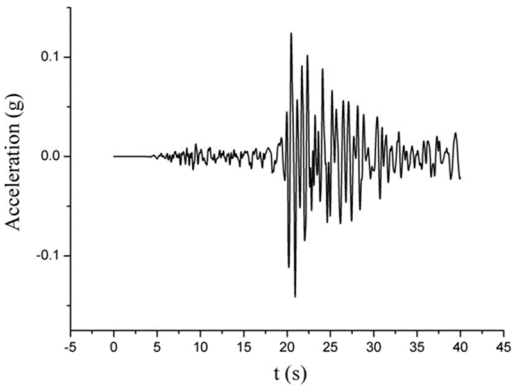

Fig. 16 1995 Kobe earthquake accelerations

During the excitation, accelerations related to the shaking table and the top of the frame are measured and stored in a specific file in the program.

k. In this step, the desired data must be saved out of the program, and the experimental test can be stopped.

3.3 Experimental and numerical results

As mentioned earlier in this chapter, the objective of the experimental test is to verify the integrity of the toggle coefficient Ω. For achieving this goal, the numerical and experimental results should be compared. However, in these two processes, the data of the results obtained are not the same kind. Furthermore, the measured data in the experimental test are made of accelerations, while those in the numerical calculations are made of the state variables, i.e., displacement and velocity. For making practical this comparison, the obtained velocities from the numerical calculation should be converted to the accelerations using the differential of the velocity in the proper time intervals. Calculation of the differences between adjacent velocities can be easily performed by the DIFF function in MATLAB® software. DIFF is a function in Matlab Software that calculates differences between adjacent

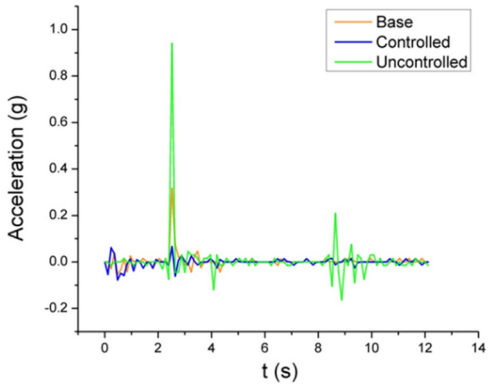

Fig. 17 Experimental results for controlled and uncontrolled system with 1979 El Centro earthquake

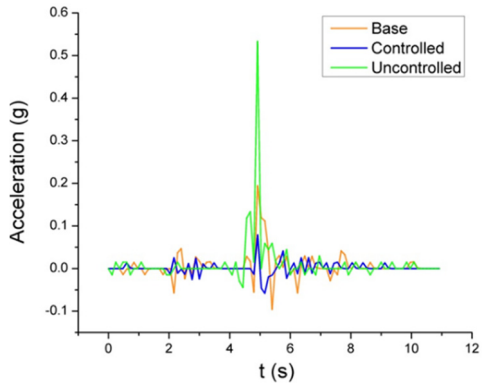

Fig. 18 Experimental results for controlled and uncontrolled system with 1992 Mendocino earthquake

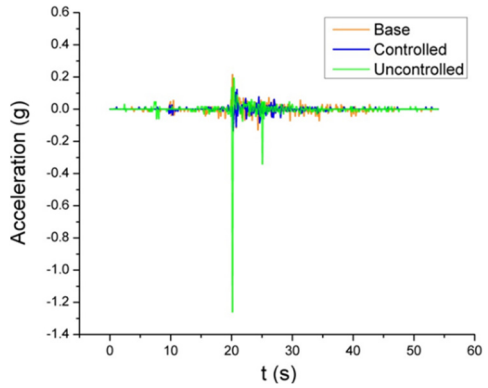

Fig. 19 Experimental results for controlled and uncontrolled system with 1995 Kobe earthquake

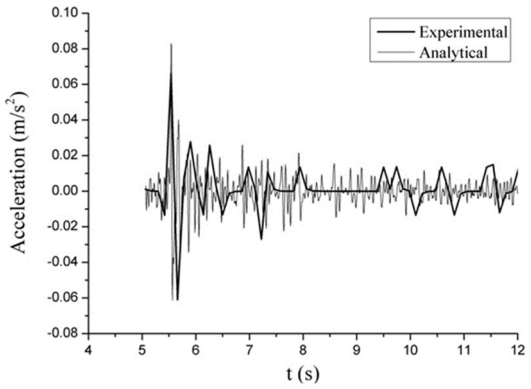

Fig. 20 Comparison between experimental and numerical results in controlled system with 1979 El Centro earthquake

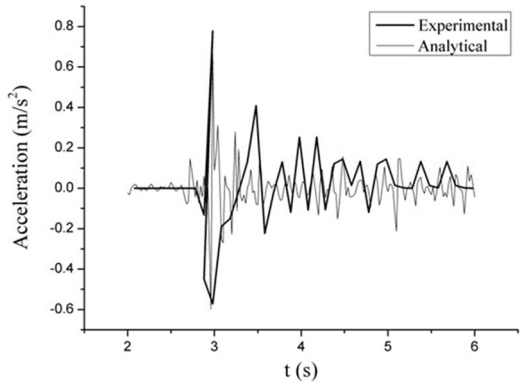

Fig. 21 Comparison between experimental and numerical results in controlled system with 1992 Mendocino earthquake

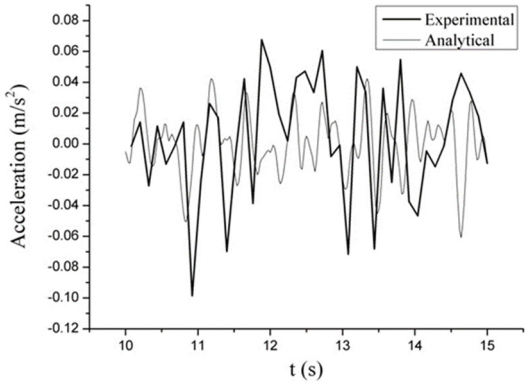

Fig. 22 Comparison between experimental and numerical result in controlled system with 1995 Kobe Earthquake

elements along with the given data. Then, both the numerical and experimental results become comparable. The controlled and uncontrolled results based on experimental and numerical results are shown in Figs. 17 to 22, respectively.

The compared results indicated in Figs. 17 to 22 show good coverage between the graphs in the experimental and numerical results. However, some inconsistencies can be seen in some areas between the compared results. The reason for this could be related to the following issues:

a. The utilized accelerometers record the accelerations in the time intervals of 0.10 to 0.12 seconds. This means that some of the encountered shaking table acceleration data cannot be measured at the right time. Consequently, the system misses the control force related to that specific time. Using more accurate accelerometers that are in harmony with the system may improve the results.
b. In this experimental environment, the only measurable and comparable parameter is system acceleration. As was explained earlier in this section, the numerical acceleration results have been derived using the velocity values gained via the LSIM function, utilizing the DIFF function in Matlab® software. This method has some inaccuracies and can cause some errors in the system. Using the bigger model and installing the proper displacement or velocity measuring devices in the system may improve the compared results. It should be noted, LSIM is a function in Matlab Software that plots the simulated time response of the dynamic system model to the input history.
c. In this experimental model, a servo motor is installed as an actuator in the system. If the experimental model is prepared in the scale close to the real system, a very fast linear actuator can be used, and the applied control forces to the system can be measured. Then, the latter experimental results can be compared with the numerical results calculated through the algorithm.

Relative errors are usually observed during comparisons of experimental and numerical results. Given the importance of this issue, some researchers have conducted significant studies in this regard. Vu-Bac et al. provide a sensitivity analysis toolbox consisting of a set of Matlab functions that offer utilities for quantifying the influence of uncertain input parameters on uncertain model outputs (Vu-Bac *et al*. 2016).

In this study, these errors have been already outlined, can be listed as below:

- Some of the encountered shaking table acceleration data cannot be measured at the right time, and the system misses the control force related to that specific time.
- In this experimental environment, the only measurable and comparable parameter is system acceleration. These acceleration data have been derived using the velocity values that can create some inaccuracies in the system.
- In this experimental model, instead of a very fast linear actuator, a servo motor has been used. The applied control forces cannot be measured and compared with the calculated forces through the algorithm.

4. Conclusions

In this study, new toggled actuator forces in active vibration control were proposed. In addition to numerical studies, experimental studies were performed to evaluate the performance of the proposed toggled actuator. The numerical studies were presented in the first part of this research. However, the experimental studies were presented in this part of the research. The results of the research are as follows:

The promising experimental results show that an active control system experimental test can be carried out by using the set of the benchtop shaking table I-40, a proper small scale frame, a suitable actuator, a controller platform named ATmega328, analogue accelerometers known as ADXL335, and the algorithm programmed in Matlab® software.

1. This experimental process is intensively economical compared with the full-scale model.
2. Using this type of experimental test can be performed in a small room and does not need a large industrial laboratory.
3. The experimental results prove the effectiveness of the toggle coefficient Ω in the reduction of the control forces in the active toggle control system.
4. The experimental results strongly verify the vibration reduction of the relevant frame under different earthquake excitations in the active toggle control system.
5. Also, the experimental results confirm the integrity of the observer technique in using the acceleration measurement to find the full-state vector in the active toggle control system.

References

Abe, M. and Fujino, Y. (1994), "Dynamic characterization of multiple tuned mass dampers and some design formulas", *Earthq. Eng. Struct. Dyn.*, **23**(8), 813-835. https://doi.org/10.1002/eqe.4290230802

Ahmadi, H.R. and Anvari, D. (2018a), "Health monitoring of pedestrian truss bridges using cone-shaped kernel distribution", *Smart Struct. Syst., Int. J.*, **22**(6), 699-709. https://doi.org/10.12989/sss.2018.22.6.699

Ahmadi, H.R. and Anvari, D. (2018b), "New damage index based on least squares distance for damage diagnosis in steel girder of bridge's deck", *Struct. Control Health Monitor.*, **25**(10), e2232. https://doi.org/10.1002/stc.2232

Ahmadi, H.R., Daneshjoo, F. and Khaji, N. (2015), "New damage indices and algorithm based on square time–frequency distribution for damage detection in concrete piers of railroad bridges", *Struct. Control Health Monitor.*, **22**(1), 91-106. https://doi.org/10.1002/stc.1662

Ahmadi, H.R., Namdari, N., Cao, M. and Bayat, M. (2019), "Seismic investigation of pushover methods for concrete piers of curved bridges in plan", *Comput. Concrete, Int. J.*, **23**(1), 1-10. https://doi.org/10.12989/cac.2019.23.1.001

Alavi, A.H., Jiao, P., Buttlar, W.G. and Lajnef, N. (2018), "Internet of Things-enabled smart cities: State-of-the-art and future trends", *Measurement*, **129**, 589-606. https://doi.org/10.1016/j.measurement.2018.07.067

Alkayem, N.F., Cao, M. and Ragulskis, M. (2019), "Damage localization in irregular shape structures using intelligent FE model updating approach with a new hybrid objective function and social swarm algorithm", *Appl. Soft Comput.*, **83**, 105604. https://doi.org/10.1016/j.asoc.2019.105604

Amini, F. and Tavassoli, M.R. (2005), "Optimal structural active control force, number and placement of controllers", *Eng. Struct.*, **27**(9), 1306-1316. https://doi.org/10.1016/j.engstruct.2005.01.006

Bagha, A.K. and Modak, S.V. (2017), "Feedback control strategies for active control of noise inside a 3-D vibro-acoustic cavity", *Smart Struct. Syst., Int. J.*, **20**(3), 273-283. https://doi.org/10.12989/sss.2017.20.3.273

Bayat, M., Bayat, M., Kia, M., Ahmadi, H.R. and Pakar, I. (2018), "Nonlinear frequency analysis of beams resting on elastic foundation using max-min approach", *Geomech. Eng., Int. J.*, **16**(4), 355-361. https://doi.org/10.12989/gae.2018.16.4.355

Bayat, M., Ahmadi, H.R. and Mahdavi, N. (2019), "Application of power spectral density function for damage diagnosis of bridge piers", *Struct. Eng. Mech., Int. J.*, **71**(1), 57-63. https://doi.org/10.12989/sem.2019.71.1.057

Bayat, M., Pakar, I., Ahmadi, H.R., Cao, M. and Alavi, A.H. (2020a), "Structural health monitoring through nonlinear frequency-based approaches for conservative vibratory systems", *Struct. Eng. Mech., Int. J.*, **73**(3), 331-337. https://doi.org/10.12989/sem.2020.73.3.331

Bayat, M., Kia, M., Soltangharaei, V., Ahmadi, H.R. and Ziehl, P. (2020b), "Bayesian demand model based seismic vulnerability assessment of a concrete girder bridge", *Adv. Concrete Constr., Int. J.*, **9**(4), 337-343. https://doi.org/10.12989/acc.2020.9.4.337

Bayramoglu, G., Ozgen, A. and Altinok, E. (2014), "Seismic performance evaluation and retrofitting with viscous fluid dampers of an existing bridge in Istanbul", *Struct. Eng. Mech., Int. J.*, **49**(4), 463-477. https://doi.org/10.12989/sem.2014.49.4.463

Bisheh, H., Wu, N. and Rabczuk, T. (2019), "Free vibration analysis of smart laminated carbon nanotube-reinforced composite cylindrical shells with various boundary conditions in hygrothermal environments", *Thin-Wall. Struct.*, **149**, 106500. https://doi.org/10.1016/j.tws.2019.106500

Braz-Cesar, M.T. and Barros, R. (2018), "Semi-active fuzzy based control system for vibration reduction of a sdof structure under seismic excitation", *Smart Struct. Syst., Int. J.*, **21**(4), 389-395. https://doi.org/10.12989/sss.2018.21.4.389

Cao, M. and Qiao, P. (2009), "Novel Laplacian scheme and multiresolution modal curvatures for structural damage identification", *Mech. Syst. Signal Process.*, **23**(4), 1223-1242. https://doi.org/10.1016/j.ymssp.2008.10.001

Cao, H., Reinhorn, A.M. and Soong, T.T. (1998), "Design of an active mass damper for a tall TV tower in Nanjing, China", *Eng. Struct.*, **20**(3), 134-143. https://doi.org/10.1016/S0141-0296(97)00072-2

Cao, M., Radzieński, M., Xu, W. and Ostachowicz, W. (2014), "Identification of multiple damage in beams based on robust curvature mode shapes", *Mech. Syst. Signal Process.*, **46**(2), 468-480. https://doi.org/10.1016/j.ymssp.2014.01.004

Cheng, F.Y. (1988), "Response control based on structural optimization and its combination with active protection", *Proceedings of the World Conference on Earthquake Engineering*, Tokyo-Kyoto, Japan.

Cheng, F.Y., Jiang, H. and Lou, K. (2008), *Smart structures: innovative systems for seismic response control*, CRC Press, Boca Raton, Florida, USA.

Chopra, A.K. (2017), *Dynamics of Structures. Theory and Applications to Earthquake Engineering*, Prentice-hall International Series, NY, USA.

Constantinou, M.C., Tsopelas, P., Hammel, W. and Sigaher, A.N. (2001), "Toggle-brace-damper seismic energy dissipation systems", *J. Struct. Eng.*, **127**(2), 105-112.

https://doi.org/10.1061/(ASCE)0733-9445(2001)127:2(105)
Council, B.S.S. (2000), *Prestandard and commentary for the seismic rehabilitation of buildings*, Report FEMA-356, Washington, DC, USA.
De Domenico, D. and Ricciardi, G. (2018), "Earthquake protection of existing structures with limited seismic joint: base isolation with supplemental damping versus rotational inertia", *Adv. Civil Eng.*, **2018**, 6019495. https://doi.org/10.1155/2018/6019495
Dinh, V.N., Basu, B. and Nagarajaiah, S. (2016), "Semi-active control of vibrations of spar type floating offshore wind turbines", *Smart Struct. Syst.*, *Int. J.*, **18**(4), 683-705. https://doi.org/10.12989/sss.2016.18.4.683
Fisco, N.R. and Adeli, H. (2011), "Smart structures: part I—active and semi-active control", *Scientia Iranica*, **18**(3), 275-284. https://doi.org/10.1016/j.scient.2011.05.034
Fu, F. (2018), *Design and Analysis of Tall and Complex Structures*, Butterworth-Heinemann, Oxford, UK.
Gandomi, A.H., Alavi, A.H. and Yun, G.J. (2011), "Nonlinear modeling of shear strength of SFRC beams using linear genetic programming", *Struct. Eng. Mech.*, *Int. J.*, **38**(1), 1-25. https://doi.org/10.12989/sem.2011.38.1.001
Gharebaghi, S.A. and Zangooei, E. (2017), "Chaotic particle swarm optimization in optimal active control of shear buildings", *Struct. Eng. Mech.*, *Int. J.*, **61**(3), 347-357. https://doi.org/10.12989/sem.2017.61.3.347
Hasni, H., Alavi, A.H., Jiao, P. and Lajnef, N. (2017), "Detection of fatigue cracking in steel bridge girders: a support vector machine approach", *Arch. Civil Mech. Eng.*, **17**(3), 609-622. https://doi.org/10.1016/j.acme.2016.11.005
He, J., Xu, Y.L., Zhang, C.D. and Zhang, X.H. (2015), "Optimum control system for earthquake-excited building structures with minimal number of actuators and sensors", *Smart Struct. Syst.*, *Int. J.*,**16**(6), 981-1002. https://doi.org/10.12989/sss.2015.16.6.981
Hejazi, F., Shoaei, M.D., Tousi, A. and Jaafar, M.S. (2016), "Analytical model for viscous wall dampers", *Comput.-Aided Civil Infrastruct. Eng.*, **31**(5), 381-399. https://doi.org/10.1111/mice.12161
Housner, G., Bergman, L.A., Caughey, T.K., Chassiakos, A.G., Claus, R.O., Masri, S.F., Skelton, R.E., Soong, T.T., Spencer, B.F. and Yao, J.T. (1997), "Structural control: past, present, and future", *J. Eng. Mech.*, **123**(9), 897-971. https://doi.org/10.1061/(ASCE)0733-9399(1997)123:9(897)
Hwang, J.S., Huang, Y.N., Hung, Y.H. and Huang, J.C. (2004), "Applicability of seismic protective systems to structures with vibration-sensitive equipment", *J. Struct. Eng.*, **130**(11), 1676-1684. https://doi.org/10.1061/(ASCE)0733-9445(2004)130:11(1676)
Hwang, J.S., Huang, Y.N. and Hung, Y.H. (2005), "Analytical and experimental study of toggle-brace-damper systems", *J. Struct. Eng.*, **131**(7), 1035-1043. https://doi.org/10.1061/(ASCE)0733-9445(2005)131:7(1035)
Ikeda, Y., Sasaki, K., Sakamoto, M. and Kobori, T. (2001), "Active mass driver system as the first application of active structural control", *Earthq. Eng. Struct. Dyn.*, **30**(11), 1575-1595. https://doi.org/10.1002/eqe.82
Kareem, A., Kijewski, T. and Tamura, Y. (1999), "Mitigation of motions of tall buildings with specific examples of recent applications", *Wind Struct.*, *Int. J.*, **2**(3), 201-251. https://doi.org/10.12989/was.1999.2.3.201
Liu, D.K., Yang, Y.L. and Li, Q.S. (2003), "Optimum positioning of actuators in tall buildings using genetic algorithm", *Comput. Struct.*, **81**(32), 2823-2827. https://doi.org/10.1016/j.compstruc.2003.07.002
Lu, Z., Li, J. and Jia, C. (2018), "Studies on energy dissipation mechanism of an innovative viscous damper filled with oil and silt", *Sustainability*, **10**(6), 1-13. https://doi.org/10.3390/su10061777
Mahdavi, N., Ahmadi, H.R. and Mahdavi, H. (2012), "A comparative study on conventional push-over analysis method and incremental dynamic analysis (IDA) approach", *Scientific Res. Essays*, **7**(7), 751-773. https://doi.org/10.5897/SRE10.042
Majeed, A.P.A. Taha, Z. Abdullah, M.A. Azmi, K.Z.M. and Zakaria, M.A. (2018), "The control of an upper extremity exoskeleton for stroke rehabilitation: An active force control scheme approach", *Adv. Robot. Res.*, *Int. J.*, **2**(3), 237-245. https://doi.org/10.12989/arr.2018.2.3.237
Miah, M.S., Chatzi, E.N. and Weber, F. (2015), "Semi-active control for vibration mitigation of structural systems incorporating uncertainties", *Smart Mater. Struct.*, **24**(5), 055016. https://doi.org/10.1088/0964-1726/24/5/055016
Mirfakhraei, S.F., Ahmadi, H.R. and Chan, R. (2020), "Numerical and experimental research on actuator forces in toggled active vibration control system (Part I: Numerical)", *Smart Struct. Syst.*, *Int. J.*, **25**(2), 229-240. https://doi.org/10.12989/sss.2020.25.2.229
Muthalif, A.G., Kasemi, H.B., Nordin, N.H., Rashid, M.M. and Razali, M.K.M. (2017), "Semi-active vibration control using experimental model of magnetorheological damper with adaptive F-PID controller", *Smart Struct. Syst.*, *Int. J.*, **20**(1), 85-97. https://doi.org/10.12989/sss.2017.20.1.085
Najafabadi, A.A., Daneshjoo, F. and Ahmadi, H.R. (2020), "Multiple damage detection in complex bridges based on strain energy extracted from single point measurement", *Frontiers Struct. Civil Eng.*, **14**, 722-730. https://doi.org/10.1007/s11709-020-0624-5
Pantelides, C.P. and Cheng, F.Y. (1990), "Optimal placement of controllers for seismic structures", *Eng. Struct.*, **12**(4), 254-262. https://doi.org/10.1016/0141-0296(90)90024-M
Park, W., Park, K.S., Koh, H.M. and Ha, D.H. (2006), "Wind-induced response control and serviceability improvement of an air traffic control tower", *Eng. Struct.*, **28**(7), 1060-1070. https://doi.org/10.1016/j.engstruct.2005.11.013
Park, W., Park, K.S. and Koh, H.M. (2008), "Active control of large structures using a bilinear pole-shifting transform with H_∞ control method", *Eng. Struct.*, **30**(11), 3336-3344. https://doi.org/10.1016/j.engstruct.2008.05.009
Rabczuk, T., Samaniego, E. and Belytschko, T. (2007), "Simplified model for predicting impulsive loads on submerged structures to account for fluid-structure interaction", *Int. J. Impact Eng.*, **34**(2), 163-177. https://doi.org/10.1016/j.ijimpeng.2005.08.012
Rao, A.R.M. and Sivasubramanian, K. (2008), "Optimal placement of actuators for active vibration control of seismic excited tall buildings using a multiple start guided neighbourhood search (MSGNS) algorithm", *J. Sound Vib.*, **311**(1-2), 133-159. https://doi.org/10.1016/j.jsv.2007.08.031
Ras, A. and Boumechra, N. (2016), "Seismic energy dissipation study of linear fluid viscous dampers in steel structure design", *Alexandria Eng. J.*, **55**(3), 2821-2832. https://doi.org/10.1016/j.aej.2016.07.012
Reinhorn, A.M., Viti, S. and Cimellaro, G. (2005), "Retrofit of structures: Strength reduction with damping enhancement", *Proceedings of the 37th UJNR Panel Meeting on Wind and Seismic Effects*.
Ricciardelli, F., Pizzimenti, A.D. and Mattei, M. (2003), "Passive and active mass damper control of the response of tall buildings to wind gustiness", *Eng. Struct.*, **25**(9), 1199-1209. https://doi.org/10.1016/S0141-0296(03)00068-3
Shokouhian, M., Shi, Y. and Head, M. (2016), "Interactive buckling failure modes of hybrid steel flexural members", *Eng. Struct.*, **125**, 153-166. https://doi.org/10.1016/j.engstruct.2016.07.001

Şigaher, A.N. and Constantinou, M.C. (2003), "Scissor-jack-damper energy dissipation system", *Earthq. Spectra*, **19**(1), 133-158. https://doi.org/10.1193/1.1540999

Soong, T.T. and Dargush, G.F. (1997), *Passive Energy Dissipation Systems in Structural Engineering*, John Wiley & Sons.

Soong, T.T. and Spencer Jr, B.F. (2002), "Supplemental energy dissipation: state-of-the-art and state-of-the-practice", *Eng. Struct.*, **24**(3), 243-259. https://doi.org/10.1016/S0141-0296(01)00092-X

Spencer Jr, B.F. and Nagarajaiah, S. (2003), "State of the art of structural control", *J. Struct. Eng.*, **129**(7), 845-856. https://doi.org/10.1061/(ASCE)0733-9445(2003)129:7(845)

Spencer, B.F. and Sain, M.K. (1997), "Controlling buildings: a new frontier in feedback", *IEEE Control Systems*, **17**(6), 19-35. https://doi.org/10.1109/37.642972

Taylor, D.P. (1999a), U.S. Patent No. 5,870,863. Washington, DC: U.S. Patent and Trademark Office.

Taylor, D.P. (1999b), U.S. Patent No. 5,934,028. Washington, DC: U.S. Patent and Trademark Office.

Tian, Z., Mokrani, B., Alaluf, D., Jiang, J. and Preumont, A. (2017), "Active tendon control of suspension bridges: Study on the active cables configuration", *Smart Struct. Syst., Int. J.*, **19**(5), 463-472. https://doi.org/10.12989/sss.2017.19.5.463

Vu-Bac, N., Lahmer, T., Zhuang, X., Nguyen-Thoi, T. and Rabczuk, T. (2016), "A software framework for probabilistic sensitivity analysis for computationally expensive models", *Adv. Eng. Software*, **100**, 19-31. https://doi.org/10.1016/j.advengsoft.2016.06.005

Xu, Y.L. and Teng, J. (2002), "Optimum design of active/passive control devices for tall buildings under earthquake excitation", *Struct. Des. Tall Build.*, **11**(2), 109-127. https://doi.org/10.1002/tal.193

Xu, H.B., Zhang, C.W., Li, H., Tan, P., Ou, J.P. and Zhou, F.L. (2014), "Active mass driver control system for suppressing wind-induced vibration of the Canton Tower", *Smart Struct. Syst., Int. J.*, **13**(2), 281-303. https://doi.org/10.12989/sss.2014.13.2.281

Yamamoto, M., Aizawa, S., Higashino, M. and Toyama, K. (2001), "Practical applications of active mass dampers with hydraulic actuator", *Earthq. Eng. Struct. Dyn.*, **30**(11), 1697-1717. https://doi.org/10.1002/eqe.88

Yamazaki, S., Nagata, N. and Abiru, H. (1992), "Tuned active dampers installed in the Minato Mirai (MM) 21 Landmark Tower in Yokohama", *J. Wind Eng. Indust. Aerodyn.*, **43**(1-3), 1937-1948. https://doi.org/10.1016/0167-6105(92)90618-K

Yang, J.N. and Soong, T.T. (1988), "Recent advances in active control of civil engineering structures", *Probabilistic Eng. Mech.*, **3**(4), 179-188. https://doi.org/10.1016/0266-8920(88)90010-0

Yanik, A. (2019), "Absolute instantaneous optimal control performance index for active vibration control of structures under seismic excitation", *Shock Vib.*, **2019**, 4207427. https://doi.org/10.1155/2019/4207427

Zhan, M., Wang, S., Yang, T., Liu, Y. and Yu, B. (2017), "Optimum design and vibration control of a space structure with the hybrid semi-active control devices", *Smart Struct. Syst., Int. J.*, **19**(4), 341-350. https://doi.org/10.12989/sss.2017.19.4.341